Graphene single-electron transistors

Graphene, a single layer of carbon atoms forming a perfectly stable and clean two-dimensional crystal with very few defects, has been proclaimed to be a new revolutionary material for electronics. These hopes rest mainly on the unique band structure properties of graphene. Although living essentially on the surface, electron mobilities in this material do not suffer extensively from surface contaminations and are surprisingly high even at room temperature. In comparison to extremely high quality semiconducting materials, such as Silicon and GaAs, the understanding of electronic transport in graphene is still in its infancy. Research on nanoscale transistors switching with only a single electron exemplifies that there are a number of unresolved problems that material scientists should tackle in the future for making the graphene dreams come true.

T. Ihn[1,*], J. Güttinger[1], F. Molitor[1], S. Schnez[1], E. Schurtenberger[1], A. Jacobsen[1], S. Hellmüller[1], T. Frey[1], S. Dröscher[1], C. Stampfer[1,2], K. Ensslin[1]

[1]Solid State Physics Laboratory, ETH Zurich, CH-8093 Zurich, Switzerland
[2]Present address: JARA-FIT and II. Institute of Physics, RWTH Aachen University, 52074 Aachen, Germany
*E-mail: ihn@phys.ethz.ch

The ubiquitous success of semiconductors in electronics relies on the tunability of their electronic properties using electric fields generated by gate electrodes. It is a direct consequence of the existence of an energy band gap separating the completely filled valence band from the empty conduction band[1]. Surprisingly, such a field effect has been also demonstrated in graphene[2], which unlike semiconductors does not have a band gap[3]. In graphene, conduction electrons form a two-dimensional gas like that found in modern Silicon field-effect transistors (FETs)[4] at the interface between silicon and the gate dielectric. In graphene, this two-dimensional electron gas has a thickness on the angstrom scale, roughly one hundred times thinner than electron gases in FETs[4]. Paired with the ease of making ohmic contacts the discovery of the field effect has sparked hopes that future nanoscale electronics could greatly benefit from this material[5,6], and it has provided fundamental research with a new interesting and unique material. Visions even extend into the realm of quantum information processing, where graphene could be the basis material for the realization of spin qubits with very long coherence times[7].

Electronic transport in bulk graphene

Like all conducting materials, bulk graphene derives its electronic properties from its band structure shown schematically in the upper inset of Fig. 1. The quantum states relevant for electrical conduction are close to the K and K' points in the k-space of the reciprocal lattice, where the energy E and the wave-vector k (the electron's momentum) have a linear relation[3]. Electrons in graphene have been called *massless Dirac fermions*[8], because such a linear energy-momentum relation is also found in relativistic quantum mechanics relevant for high-energy physics[9]. The density of states derived from this linear dispersion relation is also linear in energy[9] (see lower left inset of Fig. 1). In theory it vanishes at the energy of the K- and K'-points, where the conduction- and valence bands touch.

The field effect in graphene[2] manifests itself in the tunability of the conductance of a sheet of many square microns in size, as shown in Fig. 1. The back-gate voltage is linearly related to the charge carrier density (horizontal axis). The minimum seen in the conductance, here measured at a temperature of 2 Kelvin, marks the so-called charge neutrality point. The low-temperature conductivity σ is related to the carrier density n via Drude's formula[1] $\sigma = ne\mu$. The almost linear increase of σ on both sides of the charge neutrality point indicates that the mobility μ is independent of carrier density[2].

Close to the charge neutrality point, the density of the electron gas is believed to be very inhomogeneous[10,11]. Electrons and holes arrange themselves in puddles induced by spatial disorder. The exact origin of the disorder is still debated: possible candidates are contaminations on the surface above or below the graphene sheet[12], impurities in the
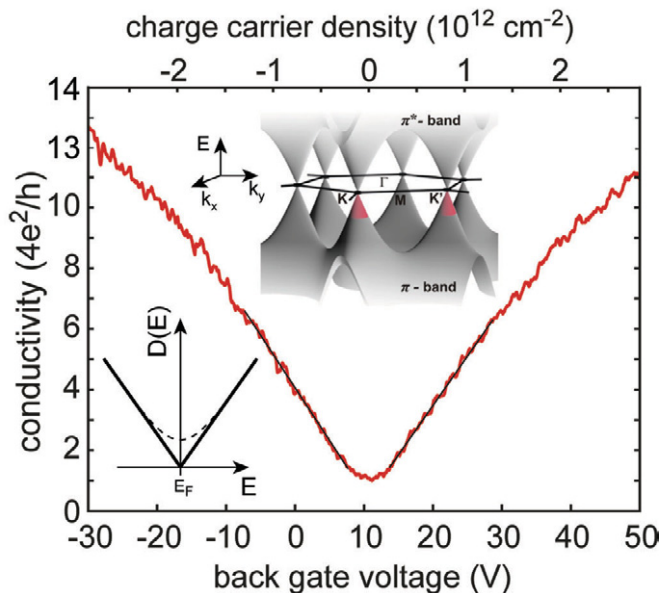

Fig. 1 Conductivity of a single layer graphene flake as a function of the back-gate voltage. The top inset shows the dispersion relation of graphene at energies where the conduction- and valence bands touch in the K and K' points. The bottom left inset is the theoretically calculated density of states (black solid line), and a density of states resulting from energy averaging caused by disorder in the system (dashed line).
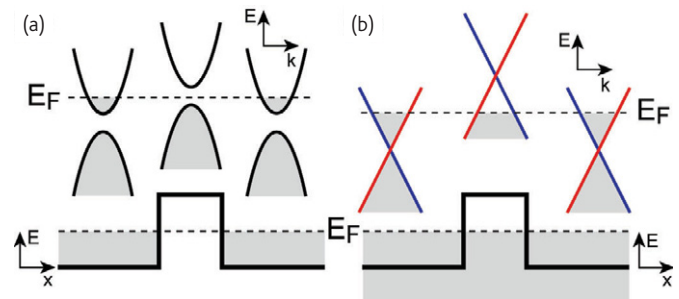

Fig. 2 Comparison of the quantum states in the presence of a rectangular potential barrier (a) in a conventional semiconductor, and (b) in graphene. At the bottom of each subfigure, a space–energy diagram is shown, whereas the top shows the wave-vector–energy dispersion relations in the region of the barrier and outside.

substrate, and warping of the sheet. There is experimental evidence that heating the devices in vacuum before measurement improves the mobility[13-15]. Experiments on suspended graphene sheets have lead to mobilities around 200 000 cm^2/Vs, the highest mobilities reported so far[16,17]. Material quality (including the substrate) is the main issue here.

Conductivities near the charge neutrality point have been experimentally found[5,18,19] to be typically around the conductance quantum $4e^2/h$. It is commonly believed that the analogue of Klein-tunneling[20] known from relativistic particle physics is responsible for the large conductivity in the inhomogeneous system[21]. Fig. 2 shows a comparison between a rectangular potential barrier in a conventional semiconductor with band gap and parabolic conduction and valence band dispersion, and graphene without band gap and linear dispersion relation. In the conventional semiconductor, no electronic states exist in the barrier region, and electrons have to tunnel from left to right. In contrast, in graphene there is no band gap, and electronic states do also exist in the barrier region. It can be shown[20] that the barrier has a finite transmission for electrons in this case.

Nanostructure fabrication

Graphene nanostructures can be fabricated on the basis of graphite mechanically exfoliated with scotch tape[2,22]. While this technique has initiated the whole field of graphene research, it is only useful for individual structures used in fundamental investigations. Advanced fabrication techniques leading to large-area monolayer coverage of a substrate would be highly desirable, and are probably decisive for the future technological use of graphene in electronics. A table with approaches that have been explored so far, ranging from mechanical exfoliation to epitaxial growth, can be found in Ref. 23.

The material deposited by mechanical exfoliation on a Si/SiO$_2$ substrate consists of many flakes that need not necessarily have the thickness of one single atomic layer. Inspection of the flakes with an optical microscope[24,28], and Raman spectroscopy[25,26] are usually used to select single-layer flakes.
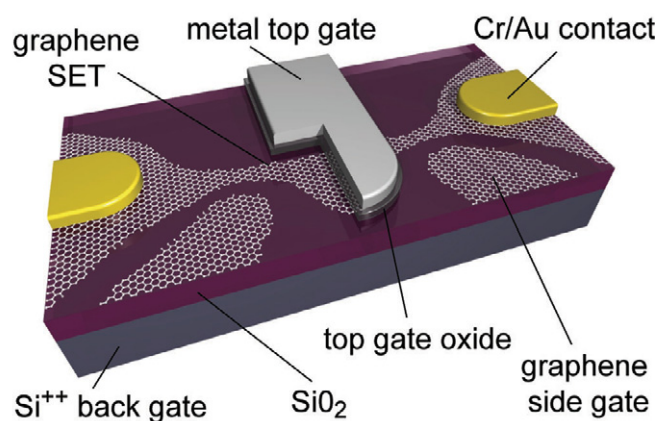
Fig. 3 Schematic drawing of a typical nanostructure made from a monolayer graphene flake. The graphene sheet is deposited on a substrate consisting of highly doped silicon (Si++ back gate) and 295 nm silicon oxide (SiO₂). Depositing a Chromium/Gold layer (Cr/Au contact) directly on the flake makes an ohmic contact. Metallic top-gates have to be separated from the flake by thin dielectric insulators (top gate oxide). In the drawing, the top-gate has been cut open in order to show the graphene structure below. In-plane gates made of graphene (graphene side gate) are obtained by etching a trench into the graphene sheet.
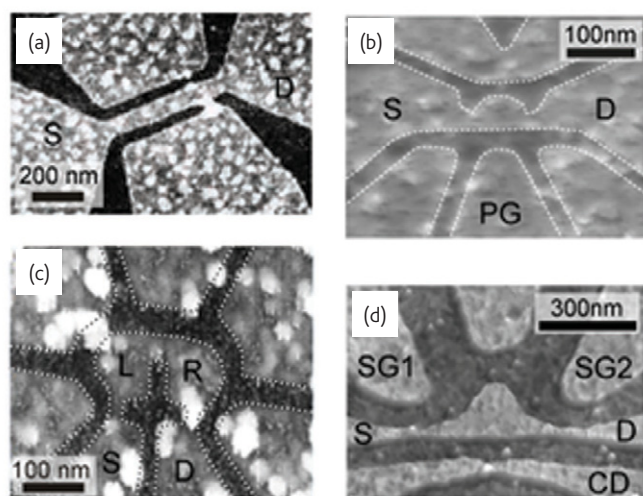

Fig. 4 Scanning force microscope images of graphene nanostructures. (a) A nanoribbon with 85 nm width and 500 nm length. (b) A single-electron transistor device with source (S) and drain (D) contacts and a number of in-plane gates (for example the plunger gate PG). (c) A device consisting of two single-electron transistors coupled in series. (d) A single-electron transistor with a graphene nanoribbons serving as an integrated charge detector (CD).

Gate electrodes needed to exploit the field effect for tuning a graphene nanostructure in situ have been either realized by using a highly doped silicon substrate isolated from the graphene sheet by a layer of SiO₂[2], by depositing a dielectric insulator and a metal on top of the sheet[27,28], or by using in-plane gates made of graphene[29,30]. Fig. 3 shows these three options schematically in three-dimensions. The highly doped Si substrate with a thermal SiO₂ oxide of about 295 nm is common to most transport experiments and allows adjusting the

overall electron density in the device[2]. In-plane gates are an easy way to tune the electronic properties locally[29,30]. They are made from the same flake as the device by etching a narrow trench in a reactive ion etching reactor after defining the corresponding resist pattern with electron beam lithography. Fig. 4 shows a number of devices with in-plane gates ranging from a narrow graphene channel[31], via single[68] and coupled[32] single-electron transistors (SETs) to an integrated circuit consisting of a constriction and an SET[33]. If top gates are used (typically fabricated with electron beam lithography techniques), careful studies have to be made how the gate insulator affects the electronic quality of the underlying graphene flake[27,28].

Confinement of electrons by electrostatic gating, a technique commonly used for semiconductor nanostructures, is not easily achieved in graphene, as a result of the lack of a band gap and the associated Klein-tunneling phenomenon described above. Therefore confinement is usually accomplished by etching trenches into graphene flakes[29,30,34,35], as shown in Figs. 3 and 4. The chemical composition and roughness of the resulting edges has remained an open question to date, and novel fabrication techniques giving finer control over the crystal orientation and smoothness of edges are certainly highly desirable for establishing a reliable graphene technology. However, alternative attempts, such as local anodic oxidation with the AFM[36,37] have had only limited success so far. Luckily, the available reactive ion etching technique has turned out to be good enough for fundamental research on graphene nanostructures.

Graphene constrictions

Narrow graphene constrictions, sometimes called nanoribbons (one of which is depicted in Fig. 4a) are the simplest building blocks for more complicated nanostructures. Early theories dating back to a time before graphene was accessible for experiments propose that the dispersion relation and density of states in perfect nanoribbons with smooth edges depend strongly on the orientation of the ribbon edge and on the ribbon width[38,39,77]. This is similar to carbon nanotubes where the electronic properties (e.g., metallic or semiconducting) depend crucially on the chirality and the diameter of the nanotubes[9,40].

As a result of the honeycomb crystal lattice there can be zigzag or armchair edges, or a combination of both[38]. Ribbons with perfect armchair edges have been predicted to exhibit a confinement-induced gap between valence- and conduction band, if the number N of dimer rows within the width of the ribbon fulfills $N \neq 3M$-1 (M is a positive integer)[38,39,77] (see the density of states depicted in Fig. 5a). If $N=3M$-1, however, the dispersion remains gapless and linear, and the density of states is constant around the charge neutrality point[38,39,77], as shown in Fig. 5b. In contrast, ribbons with perfect zigzag edges are predicted to be gapless and to form edge states that lead to a peak in the density of states at the charge neutrality point (Fig. 5c)[38,39,77]. If a combination of zigzag and armchair edges arises, edge states can survive, but tend to localize along the ribbon edge[38,41-43]. Edge
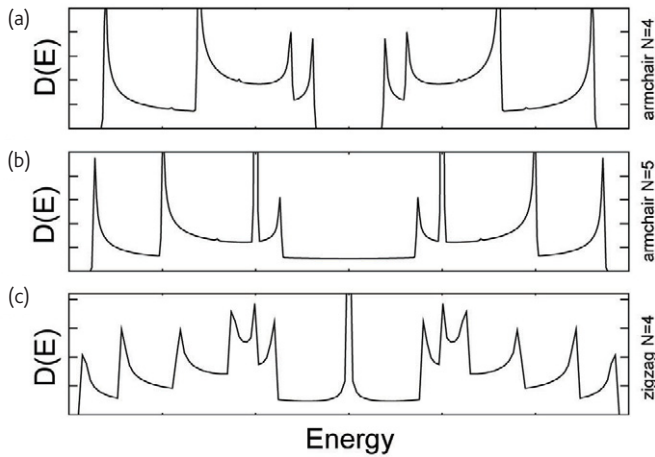
Fig. 5 Theoretically calculated densities of states of graphene nanoribbons (courtesy of Katsunori Wakabayashi, see also[77]). (a) Density of states of a nanoribbons with armchair edges and an N=4 dimer rows across its width exhibiting a band gap. (b) The same as (a) with N=5 dimer rows. (c) Density of states of a nanoribbon with zigzag edges.

states have been recently investigated experimentally using scanning tunneling microscopy[44,45].

Starting from the early predictions[38,39], experimentalists have been keen to find out, if the confinement in narrow ribbons can really induce a band gap that would facilitate further electrostatic confinement of electrons along the nanoribbon axis[31,34,46-51]. Fig. 6a shows the measured low-temperature (T = 2 K) conductance of a typical device as a function of back-gate voltage (or electron density). Indeed the conductance is found to be markedly different from the conductivity of the bulk material shown in Fig. 1. First of all, the curve shows very strong fluctuations of the conductance as a function of V_{BG}. These are stable in time and reproducible in successive measurements on the same sample. Second, there is a region of back-gate voltage between -1 and -4 V where the conductance is strongly suppressed (the term "transport gap" has been used to describe this region[46]). However, even in this region strong resonances occur. This behavior is in marked difference to constrictions in high-quality two-dimensional electron gases in semiconductors, where conductance quantization is routinely observed at low temperatures[52].
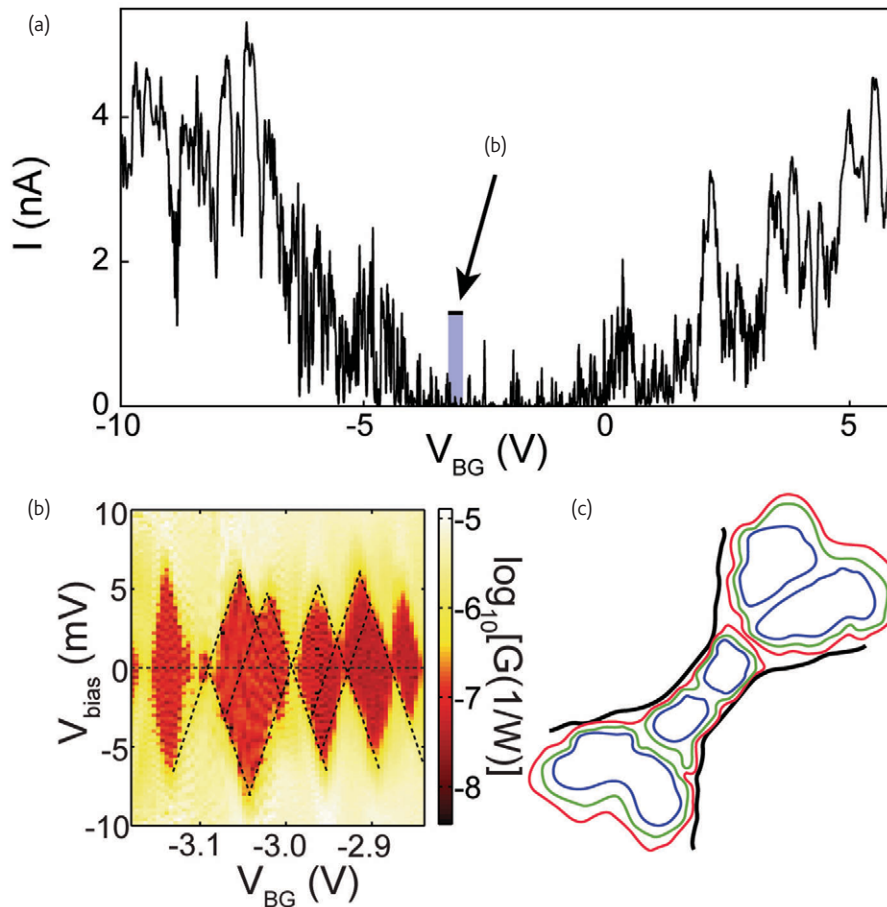

Fig. 6 (a) Conductance of a 85 nm wide and 500 nm long nanoribbon measured as a function of the back-gate voltage. The ribbon was fabricated by electron beam lithography and subsequent reactive ion etching. (b) Conductance measured as a function of back-gate voltage and source-drain bias voltage in the region of strongly suppressed conductance in (a). Pronounced Coulomb blockade diamonds can be seen. (c) Schematic representation of a generic localization–delocalization transition driven by an interplay of disorder and interaction.
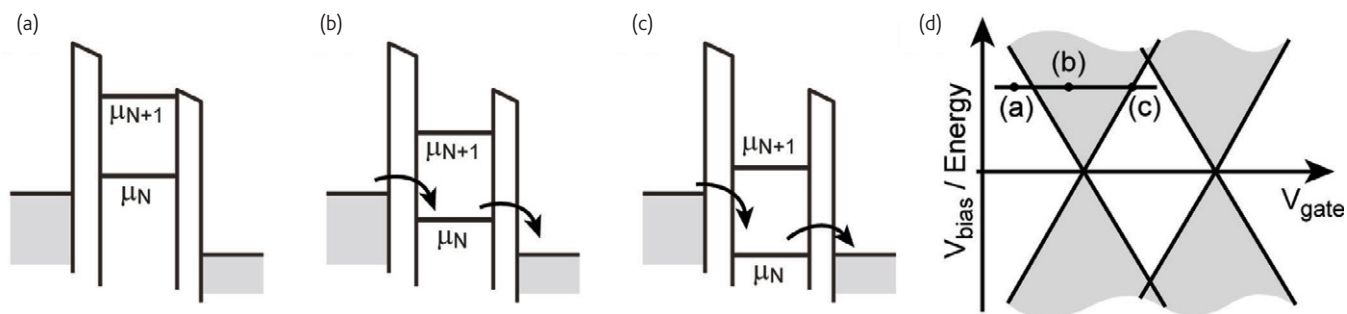
Fig. 7 (a-c) Space–energy diagrams of a single-electron transistor in which electrons are confined between two tunneling barriers. The plunger gate voltage is increased from (a) to (c). (d) Current can flow only in the gray-shaded regions, where one of the energy levels is within the bias window.

Details about the origin of the suppressed conductance can be investigated by measuring the conductance in a very narrow range of back-gate voltages also as a function of the applied source–drain bias voltage[46,47]. The result of such a measurement is shown in Fig. 6b. The figure reveals diamond-shaped regions of completely suppressed conductance (red) mutually connected by sharp resonances at zero bias voltage. Such diamonds are known from electronic transport through single-electron transistors (SETs) in the Coulomb-blockade regime[53].

Fig. 7 illustrates how the Coulomb blockade phenomenon comes about in SETs. An SET is a structure in which electrons are spatially confined. Tunneling barriers connect the SET weakly to source and drain leads. The addition of each extra electron to the SET requires a classical charging energy e^2/C (C is the quantum dot's capacitance). This leads to a ladder of discrete addition levels μ_N indicating the energy required to add the Nth electron. These levels can be shifted up or down in energy by applying a voltage to the plunger gate of the SET. At low temperatures ($k_BT \ll e^2/C$) and a given finite source–drain bias-voltage, current can only flow, if one of these levels is shifted through the bias window by sweeping the plunger gate voltage. If no level is in the bias window, the current is blocked as a result of the Coulomb interaction between electrons (Coulomb blockade). As illustrated in Fig. 7d, for each μ_N the range of plunger gate voltages where current can flow increases linearly with increasing source–drain bias voltage. Arranging a sequence of such double-triangles along the plunger gate axis leads to the observed Coulomb blockade diamonds.

It is believed that the "SETs" leading to the observed Coulomb blockade diamonds in Fig. 6b form spontaneously in the nanoribbons as a result of spatial potential variations and edge roughness. Recent theoretical models based on non-interacting electrons have demonstrated that edge roughness and bulk disorder lead to Anderson-localization of states[41-43,54,55]. The observation of Coulomb blockade phenomena indicates that also electron-electron interaction and screening play an important role for the formation of these localized states[56]. One particular model based on a self-consistent percolation analysis explains the formation of electron- and hole-puddles and predicts a percolation driven metal-insulator transition[57]. Figure 6c shows a schematic illustration of such a transition. Starting in a region where the conductance is strongly suppressed, several localized electron or hole puddles exist (regions encircled in blue). If the electron density is increased, some of these puddles can merge (regions encircled in green). Eventually, the constriction becomes almost transparent and all short scale localized puddles have merged into big conducting regions (regions encircled in red).
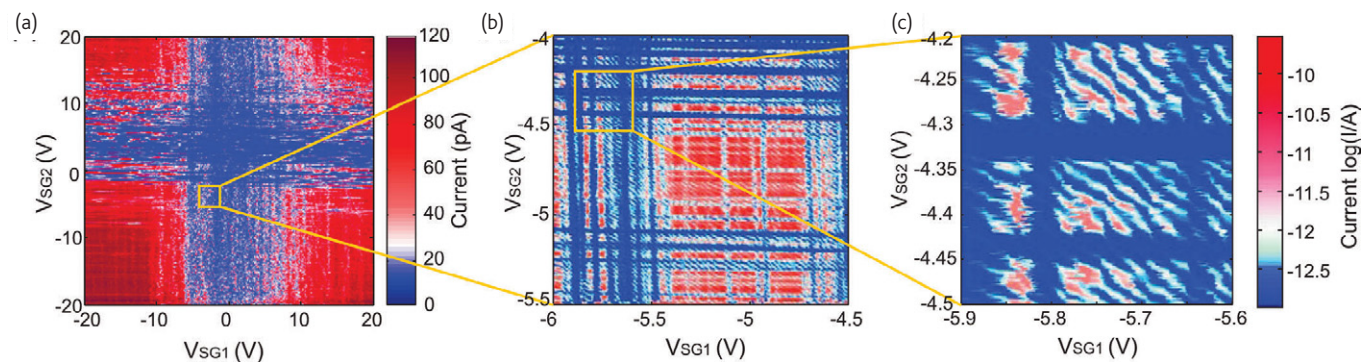

Fig. 8 Conductance of a graphene single-electron transistor device measured as a function of the voltages applied to the two side gates tuning the constrictions. (a) Conductance in a large side gate voltage range. Regions can be identified, where the two constrictions suppress the conductance strongly. (b) Zoom into a small part of this region. Vertical and horizontal stripes of suppressed conductance originate from localization of states in the constrictions. (c) A further zoom unravels the presence of diagonal resonances running from the top left to the bottom right which are attributed to Coulomb blockade in the graphene island between the two constrictions. (b) and (c) share the colorbar on the right.
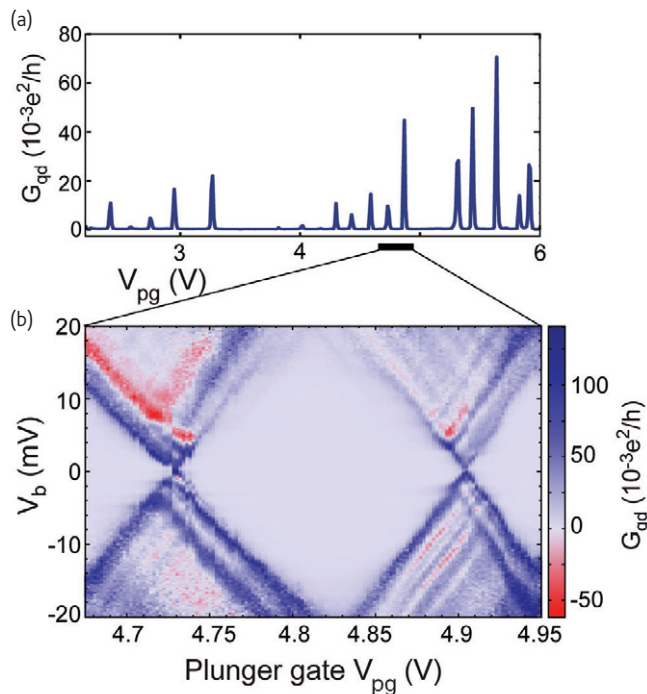
Fig. 9 (a) Conductance resonances as a function of the plunger gate voltage in a graphene quantum dot. (b) Coulomb blockade diamond measured in a graphene quantum dot as a function of plunger gate and source–drain voltage[78].

Single-electron transistors

As mentioned above, SETs consist of a small sub-micron sized island coupled weakly to source and drain contacts[53]. Bound states in narrow graphene ribbons have been discussed theoretically for different boundary conditions[58,59]. Fig. 4b shows an experimental device in which a graphene island with a size below 100 nm is coupled via two graphene constrictions to wide graphene contact regions[68]. Having discussed the strong influence of inhomogeneities and the Coulomb blockade effect in constrictions above, the question arises, if it is at all possible to observe a clear Coulomb blockade effect originating from charging the graphene island in such a structure. Indeed it has been shown in experiments[30,35,46,60,61] that the understanding of the constrictions developed above, paired with a careful analysis of the experiments, allows the unambiguous observation of the Coulomb blockade phenomenon related to the island[61].

Fig. 8a shows the conductance of such an SET device as a function of the voltages on the two in-plane gates placed close to the two constrictions (see Fig. 4d for a similar structure, side gates are labeled SG1 and SG2). The blue cross of suppressed conductance originates from the two constrictions. Each constriction exhibits a transport gap that is only tuned by the closer in-plane gate. Zooming in Fig. 8a into a smaller gate voltage region where the conductance in both constrictions is suppressed, a pronounced pattern of horizontal and vertical stripes can be seen (Fig. 8b). They originate from the

reproducibly modulated transmission of the respective constrictions. A further zoom into an even smaller region of this plot is shown in Fig. 8c. Here, a new type of resonances becomes visible running from the top left to the bottom right. This orientation of the resonances indicates that the underlying states are tuned with similar strength by both constriction gates. Geometrically, these states are therefore located on the island, which has the same distance from the two gates.

If the conductance is measured at a very small source–drain voltage ($V_{SD} \ll k_B T$), transport is only possible in an energy window of size $k_B T$ given by temperature[53]. In Fig. 9a the series of conductance resonances measured in the Coulomb-blockade regime as a function of the plunger gate voltage resembles the ladder of states μ_N, the so-called addition spectrum. Corresponding Coulomb-blockade diamonds such as those shown in Fig. 9b have by now been observed in a number of research labs worldwide[30,35,48,60,62].

The observation of the Coulomb blockade effect in graphene has paved the way for further investigations of quantum states and quantum confinement. Resonances running in parallel to the Coulomb blockade diamond boundaries seen in Fig. 9b are first indications for the importance of size quantization in these structures, and the possibility of the investigation of excited state spectra[63]. Once size quantization becomes important, physicists use the term "quantum dot" instead of "single-electron transistor". Future challenges in this field of research are the identification of spin states, and the experimental determination of the *g*-factor of graphene[64]. For example, theoretical calculations exist predicting spin polarization of edge states in graphene at zero magnetic field[65-67]. Another open question is related to the spin- and valley degeneracies in bulk graphene. In carbon nanotubes, shell filling has been observed with a four-fold filling periodicity corresponding to the two-fold spin and the two-fold valley degeneracy. In graphene, no such shell filling has been observed so far. A related aspect is the crossover from electron- to hole-confinement in graphene, where first experiments have been reported[68], but the quality of the data still remains far behind corresponding measurements in carbon nanotubes[69].

Improvements in material quality will be crucial for all these experiments and related future progress in the field, as they would reduce the influence of disorder-induced effects that are limiting experiments today. Only then will it be possible to tackle even more advanced concepts of information processing schemes with spin-qubits in graphene quantum dots that have been theoretically proposed[7]. One first experiment in this direction is the demonstration of an integrated graphene charge-readout[33] as it is known from the well-established Ga[Al]As systems[70] (see Fig. 4d). Other experiments have recently demonstrated that systems of coupled quantum dots (see Fig. 4c) can be successfully fabricated and investigated with present material quality and technology[32,71]. Such systems may in the future allow scientists to observe effects like the spin-blockade, and to implement coherent spin-manipulation techniques, again known from Ga[Al]As research already[72,73]. However, graphene is predicted to offer

major advantages compared to this well established material system: quantum decoherence due to nuclear spins and spin orbit interaction, which limit the performance of GaAs spin-qubits today, is expected to be significantly reduced in graphene where the density of nuclear spins is very small and spin-orbit interaction is supposedly weak[7].

Conclusion

Research on graphene nanostructures started a few years ago. Significant progress has been made in the field within this short time, but it seems to be only the very beginning of further exciting developments in the direction of fundamental aspects of quantum transport in graphene, and of graphene electronics for applications. Already today, bilayer graphene is being heavily investigated in research labs, because this material promises a band gap tunable by electrostatic gates[28,74]. Further interesting prospects may be graphene devices with superconducting[75] or ferromagnetic[76] contacts. Therefore there is a lot of hope that graphene research is more than a fashion in physics and materials research. Advances in material quality and fabrication techniques must be seen as the key issue, eventually deciding about the future of graphene in science and technology. mt

REFERENCES

1   Ashcroft, N. W., and Mermin, N. D., *Solid State Physics* (2008) Brooks/Cole, Belmont.

2   Novoselov, K. S., et al., *Science* (2004) **306**, 666.

3   Wallace, P. R., *Phys. Rev.* (1947) **71**, 622.

4   Ando, T., et al., *Rev. Mod. Phys.* (1982) **54**, 437.

5   Geim, A. K., Novoselov, K. S., *Nature Materials* (2007) **6**, 183.

6   Berger, C., et al., *Science* (2006) **312**, 1191.

7   Trauzettel, B., et al., *Nature Physics* (2007) **3**, 192.

8   Novoselov, K. S., et al., *Nature* (2005) **438**, 197.

9   Ando, T., *J. Phys. Soc. Jpn.* (2005) **74**, 777.

10 Martin, J., *Nature Physics* (2008) **4**, 144.

11 Hwang, E. H., et al., *Phys. Rev. Lett.* (2007) **98**, 186806; Nomura, K., and MacDonald, A. H., *Phys. Rev. Lett.* (2007) **98**, 076602; Aleiner, I. L., and Efetov, K. B., *Phys. Rev. Lett.* (2006) **97**, 236801.

12 Schedin, F., et al., *Nat. Mater.* (2007) **6**, 652.

13 Ishigami, M., et al., *Nano Lett.* (2007) **7**, 1643.

14 Stolyarova, E., et al., *Proc. Natl. Acad. Sci. USA* (2007) **104**, 9209.

15 Moser, J., et al., *Appl. Phys. Lett.* (2007) **91**, 163513.

16 Du, X., et al., *Nature Nanotechnol.* (2008) **3**, 491.

17 Bolotin, K. I., et al., *Solid State Commun.* (2008) **146**, 351.

18 Jang, C., et al., *Phys. Rev. Lett.* (2008) **101**, 146805.

19 Chen, J.-H., et al., *Phys. Rev. Lett.* (2009) **102**, 236805.

20 Katsnelson, M. I., et al., *Nature Physics* (2006) **2**, 620.

21 Katsnelson, M. I., *Materials Today* (2007) **10**, 20.

22 Novoselov, K. S., et al., *Proc. Natl. Acad. Sci. USA* (2005) **102**, 10451.

23 Taghioskoui, M., *Materials Today* (2009) **12**, 34.

24 Blake, P., et al., *Appl. Phys. Lett.* (2007) **91**, 063124; Abergel, D. S. L., et al., *Appl. Phys. Lett.* (2007) **91**, 063125.

25 Ferrari, A. C., et al., *Phys. Rev. Lett.* (2006) **97**, 187401.

26 Graf, D., et al., *Nano Lett.* (2007) **7**, 238.

27 Huard, B., et al., *Phys. Rev. Lett.* (2007) **98**, 236803.

28 Oostinga, J. B., et al., *Nature Materials* (2008) **7**, 151.

29 Molitor, F., et al., *Phys. Rev. B* (2007) **76**, 235321.

30 Stampfer, C., et al., *Appl. Phys., Lett.* (2008) **92**, 012102.

31 Molitor, F., et al., *Phys. Rev. B* (2009) **79**, 075426.

32 Molitor, F., et al., *Appl. Phys. Lett.* (2009) **94**, 222107.

33 Güttinger, J., et al., *Appl. Phys. Lett.* (2008) **93**, 212102.

34 Han, M. Y., et al., *Phys. Rev., Lett.* (2007) **98**, 206805.

35 Ponomarenko, L. A., et al., *Science* (2008) **320**, 356.

36 Giesbers, A. J. M., et al., *Solid State Commun.* (2008) **147**, 366.

37 Weng, L., et al., *Appl. Phys. Lett.* (2008) **93**, 093107.

38 Nakada, K., et al., *Phys. Rev. B* (1996) **54**, 17954.

39 Wakabayashi, K., *Phys. Rev. B* (1999) **59**, 8271.

40 Reich, S., et al., *Carbon Nanotubes* (2004) Wiley-VCH, Weinheim.

41 Gunlycke, D., et al., *Appl. Phys. Lett.* (2007) **90**, 142104.

42 Lherbier, A., et al., *Phys. Rev. Lett.* (2008) **100**, 036803.

43 Evaldsson, M., et al., *Phys. Rev. B* (2008) **78**, 161407(R).

44 Kobayashi, Y., et al., *Phys. Rev. B* (2006) **73**, 125415.

45 Niimi, Y., et al., *Phys. Rev. B* (2006) **73**, 085421.

46 Stampfer, C., et al., *Phys. Rev. Lett.* (2009) **102**, 056403.

47 Todd, K., et al., *Nano Lett.* (2009) **9**, 416.

48 Liu, X., et al., *Phys. Rev. B* (2009) **78**, 161409R.

49 Gallagher, P., et al., arXiv:0909.3886.

50 Han, M. Y., et al., arXiv:0910.4808.

51 Lin, Y. -M., et al., *Phys. Rev. B* (2008) **78**, 161409R.

52 van Wees, B. J., et al., *Phys. Rev. Lett.* (1988) **60**, 848; Wharam, D. A., et al., *J. Phys. C* (1988) **21**, L209.

53 Ihn, T., *Semiconductor Nanostructures: Quantum States and Electronic Transport* (2009), Oxford University Press

54 Querlioz, D., et al., *Appl. Phys. Lett.* (2008) **92**, 042108.

55 Mucciolo, E. R., et al., *Phys. Rev. B* (2009) **79**, 075407.

56 Sols, F., et al., *Phys. Rev. Lett.* (2007) **99**, 166803.

57 Adam, S., et al., *Phys. Rev. Lett.* (2008) **101**, 046404.

58 Silvestrov, P. G., and Efetov, K. B., *Phys. Rev. Lett.* (2007) **98**, 016802.

59 Wang, Z. F., et al., *Appl. Phys. Lett.* (2007) **91**, 053109.

60 Bunch, J. S., et al., *Nano Lett.* (2005) **5**, 287.

61 Stampfer, C., et al., *Nano Lett.* (2008) **8**, 2378.

62 Moser, J., and Bachtold, A., *Appl. Phys. Lett.* (2009) **95**, 173506.

63 Schnez, S., et al., *Appl. Phys. Lett.* (2009) **94**, 012107.

64 Lundeberg, M. B., and Folk, J. A., *Nature Physics* (2009) **5**, 894.

65 Fujita, M., et al., *J. Phys. Soc. Jpn.* (1996) **65**, 1920.

66 Okada, S., and Oshiyama, A., *J. Phys. Soc. Jpn.* (2003) **72**, 1510.

67 Kumazaki, H., and Hirashima, D. S., *J. Phys. Soc. Jpn.* (2009) **78**, 094701.

68 Güttinger, J., et al., *Phys. Rev. Lett.* (2009) **103**, 046810.

69 Jarillo-Herrero, P., et al., *Nature* (2004) **429**, 389.

70 Elzerman, J. M., et al., *Phys. Rev. B* (2003) **67**, 161308(R).

71 Moriyama, S., et al., *Nano Lett.* (2009) **9**, 2891.

72 Petta, J. R., et al., *Science* (2005) **309**, 2180.

73 Koppens, F. H. L., et al., *Nature* (2006) **442**, 766.

74 Zhang, Y., et al., *Nature* (2009) **459**, 820.

75 Heersche, H. B., et al., *Nature* (2007) **446**, 56.

76 Trbovic, J., et al., *APS March Meeting*, New Orleans, Lousiana (2008).

77 Wakabayashi, K., et al., *New J. Phys.* (2009) **11**, 095016.

78 Güttinger, J., et al., *Phys. Status Solidi B* (2009) **11-12**, inside back cover.